



ISSN 2231-3478

(Print)

JUSPS-B Vol. 37(1), 1-11 (2025). Periodicity-Monthly

Section B

(Online)



ISSN 2319-8052



Estd. 1989

JOURNAL OF ULTRA SCIENTIST OF PHYSICAL SCIENCES

An International Open Free Access Peer Reviewed Research Journal of Physical Sciences

website:- www.ultrascientist.org**Nanocrystalline Perovskites: Synthesis, Properties, and Emerging Applications**BHUPENDRA SINGH¹, LALIT KUMAR^{*2} and GAURAV JOSHI³¹Department of Physics, Ch. Chhotu Ram (P.G.) College, Muzaffarnagar, 251001 India²Department of Physics, Meerut College, Meerut, 250001 India³Department of Applied Science and Humanities, Invertis University Bareilly, 243006 IndiaCorresponding Author Email: - lalitksuvaksh@gmail.com<http://dx.doi.org/10.22147/jusps-B/370101>

Acceptance Date 31st May, 2025,

Online Publication Date 04th June, 2025

Abstract

Nanocrystalline perovskite materials, particularly rare-earth manganites of the general formula $RE_{1-x}AE_xMnO_3$ (where RE is a rare-earth element and AE is an alkaline-earth element), have garnered significant attention due to their rich structural, electronic, and magnetic phase behavior. These multifunctional materials exhibit fascinating properties such as colossal magnetoresistance (CMR), charge ordering, orbital ordering, and phase separation, making them attractive candidates for both fundamental research and technological applications. With the advent of nanoscience, the nanoscale versions of these perovskites have shown dramatically enhanced properties compared to their bulk counterparts, driven by reduced dimensionality, quantum confinement, and high surface-to-volume ratios. Various synthesis methods such as sol-gel, hydrothermal, and chemical precipitation have enabled the controlled fabrication of perovskite nanostructures including nanoparticles, nanowires, and nanotubes. Comprehensive characterization using techniques like XRD and FE-SEM reveals size- and strain-dependent evolution of structural and magnetic phases, which play a pivotal role in defining their functional behavior. These nanocrystalline perovskites exhibit promising applications in fields such as photocatalysis, sensing, and light-emitting diodes (LEDs), owing to their tunable bandgap, high photoluminescence, and exceptional charge transport properties. This review aims to provide an in-depth overview of the synthesis strategies, structural and physicochemical properties, and emerging applications of nanostructured perovskites, along with identifying key challenges and potential directions for future research.

Key words : Rietveld refinement, Sol-gel, Manganite, Ferromagnetic, Antiferromagnetic.

1- Introduction

The multifunctional perovskite materials like rare earth-manganese oxides and their multidimensional doped versions, popularly called manganites, have been the centre of attraction for nearly three decades¹⁻³. Although the practical applications of these materials remain far away from the initial expectations, their unique electronic phase profile, as seen on the composition-temperature phase diagrams, which embodies multiple electronic orders, has been the driving force for the researchers. The coexistence of multiple electronic phases has been manifested through the phenomenon of phase separation, which is now recognized as the core aspect of the manganite physics^{2,4-6}. The most attractive explicit signature of phase separation embodying manganites has been the colossal magnetoresistance (CMR).

These materials represented by $\text{RE}_{1-x}\text{AE}_x\text{MnO}_3$ (RE is a rare earth element, and AE is an alkaline earth element) offer chemical flexibility that allows the relationship between the structural, electronic, and magnetic properties of these oxides to be examined (i) over a wide range of carrier concentrations, (ii) electron as well as hole doping, (iii) under varying degree of the internal strain^{2,3}, which led to the understanding of various physical phenomena spread over a wide range of the x - T phase diagram and that make these compounds interesting so much so that even after almost 28 years into the second inning, these materials continue to attract the research community. Among these, the prominent phenomena have been the ferromagnetic (AM) double exchange (DE), antiferromagnetic (AFM) super-exchange (SE) colossal magnetoresistance (CMR), charge ordering (CO), Jahn-Teller distortion, and orbital ordering (OO)^{1-3,7-9}. Their rich electronic phase diagrams reflect the fine balance of interactions that determine the electronic ground state. These compounds represent an important aspect of condensed matter physics research. The structure, fundamental aspects, and properties of perovskite manganite materials are discussed in the first few sections of this chapter.

Nanoscience and technology is a broad and interdisciplinary area of research and development activities have been increasing worldwide in the recent decade^{10,11}. Perovskites with features on the scale of nanometer often have properties dramatically different from their bulk scale counterparts^{12,13}. The study of nanostructured materials requires a multidisciplinary approach with inspiring technological promise, involving novel synthesis and an understanding of physics and surface science¹⁴. Recently, efforts have been made to synthesize and characterize the properties of nanostructured perovskites in different forms with at least one dimension between 1 - 100 nm, such as nanoparticles^{15,16}, nanocubes¹⁷, nanorods¹⁸, nanobelts¹⁹, nanosheets²⁰, nanowires²¹, and nanotubes²² to explore the distinctive physical properties for potential applications in nanodevices²³. The effect of reducing the physical size of materials is of great importance from both fundamental considerations and modern practice¹³. Magnetic nanoparticles show specific properties such as coercivity²⁴ and superparamagnetism²⁵, which are attributed to reduced dimensions. CMR effect in these perovskite manganite materials has created an interest in regard to the electronic, structural, and magnetic properties of these materials completely. Depending on the chemical composition/divalent doping and carrier concentration (x), these perovskite manganite materials show coupled ferromagnetism and metallic behavior in the lower temperature regime, while at high temperatures, they show paramagnetic-

insulator (PMI) behavior.

The primary objective of this review is to provide a comprehensive overview of nanocrystalline perovskite materials, focusing on their synthesis strategies, structural and physicochemical properties, and recent advancements in emerging applications. This article aims to critically evaluate various synthetic routes for producing nanocrystalline perovskites, analyze the influence of nano-structuring on their functional properties, and highlight their roles in cutting-edge applications such as photovoltaics, photocatalysis, sensors, and energy storage systems. Furthermore, the review seeks to identify key challenges and suggest future directions for research in this rapidly growing field.

2- Synthesis Techniques:

2.1. Sol-gel chemical route method :

In the material science area, the Sol-gel chemical route method is the highly used damp chemical technique. In this technique, the essential yield materials are acquired from the solution by gelation. It is feasible to acquire novel yield materials because of high homogeneity of ingredient elements and intermediate preparation temperatures, which is not obtainable by other methods. This method especially includes a transition of the materials from liquid sol into the extremely sticky mass (gel). This method has a lot of benefits. High sanctity materials can be synthesized because of the convenience of the sanctification of liquids. The blending at the molecular level takes place which leads to better chemical homogeneity.

2.2. Hydrothermal method :

Reactions in hydrothermal method are carried out in autoclave, which is a pressurized sealed vessel. Water is used as a solvent and the reaction temperature is kept over the boiling point of water. Hydrothermal method exhibit following advantages: (i) water is non-toxic, a low cost solvent and eco-friendly as compared to other organic solvent (ii) lots of inorganic salts are water soluble, (iii) the stronger polarity of water can be helpful for the nanocrystals to have specific orientation during their growth and (iv) the growth of the final nanocrystals can be easily adjusted by introducing small coordinating molecules.

2.3. Chemical precipitation method :

Chemical precipitation synthesis is analogous to the hydrothermal method except the fact that the chemical reactions are performed at a moderately low reaction temperature in an open container. Reactions between the precursors in suitable solvent take place during the synthesis process. Precipitation of the nanoparticles may occur via homo or heterogeneous nucleation. Once the nuclei are formed, growth may proceed by diffusion. The reaction parameters like reactant activity, pH, temperature and the presence of catalyst can be controlled to obtain a desired growth rate and particle size.

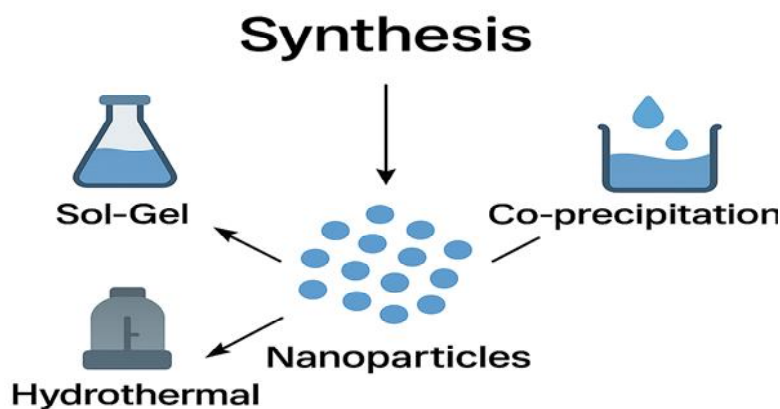


Fig. 1. Schematic representation of common synthesis methods for nanoparticles.

3- Characterization Techniques :

3.1. X-ray diffraction (XRD) :

X-ray diffraction (XRD) is one of the extremely used, powerful, and non-exterminatory technique for analysing crystalline materials. XRD technique is employed from long time to investigate the crystal structure, crystallite size, phase analysis, structural imperfections, lattice constants, and in addition, other structural characters of crystalline materials. X-rays are electromagnetic radiations that have wavelength approximately in 1-100 Å range, which is the smaller from the wavelength of visible light (3000-8000 Å). Therefore, X-rays are much penetrating and useful to see the crystal lattice. In the crystalline structure, the periodic order of the atoms could be presumed as scattering centres for the X-rays.

D.S. Raghav et al. synthesized nanocrystalline $\text{La}_{0.30}\text{Pr}_{0.30}\text{Ca}_{0.40}\text{MnO}_3$ (LPCMO) using the sol-gel method and studied the effect of sintering temperature (600/ °C, 900/ °C, 1100/ °C, and 1300/ °C) on its structural properties²⁶. Powder X-ray diffraction (XRD) patterns, analyzed via Rietveld refinement, confirmed that all samples crystallize in an orthorhombic structure with Pnma space group. With increasing sintering temperature, the average crystallite size increased from 19/ nm to 31/ nm, and the particle size ranged from 54/ nm to 457/ nm. A concurrent increase in lattice parameters, Mn–O bond lengths, and Mn–O–Mn apical bond angles was observed, indicating improved structural symmetry and reduced octahedral distortion at higher temperatures. These structural changes suggest enhanced stability and a reduction in Jahn–Teller distortion in highly sintered samples.

S.S. Kekade et al. synthesized nanocrystalline $\text{La}_{0.5}\text{Ca}_{0.5}\text{MnO}_3$ (LCMO) via the citrate gel method and confirmed its orthorhombic perovskite structure (Pnma space group) through Rietveld-refined XRD analysis, reporting lattice parameters $a = 5.426 \text{ Å}$, $b = 7.675 \text{ Å}$, and $c = 5.415 \text{ Å}$, with an average crystallite size of 35–40 nm²⁷. Similarly, W. Xia et al. prepared $\text{La}_{0.7}\text{Ca}_{0.3}\text{MnO}_3$ nanoparticles by a sol-gel route and found that all samples crystallized in a single-phase orthorhombic perovskite structure; the crystallite size increased with annealing temperature from 15 nm to 26 nm, accompanied by a shift in the (200) peak due to lattice expansion and Jahn–Teller distortion²⁸. Furthermore, Subarna

Datta et al. synthesized $\text{La}_{0.5}\text{Ca}_{0.5}\text{MnO}_3$ nanowires using a hydrothermal method and confirmed the phase purity and crystal structure through synchrotron XRD followed by Rietveld refinement, showing that the nanowires possess distorted perovskite structures correlated with MnO_6 octahedral arrangements²⁹. These studies collectively demonstrate how synthesis method, composition, and thermal treatment influence the crystallinity, particle size, and lattice structure of nanocrystalline LCMO perovskites.

3.2. FE-SEM Analysis of Perovskite Manganites :

Field Emission Scanning Electron Microscopy (FE-SEM) has proven to be an indispensable tool for characterizing the surface morphology, particle size, and microstructural evolution of perovskite manganites with high spatial resolution. Several studies have highlighted how synthesis conditions and compositional tuning critically influence morphological features, which in turn affect the physical properties of these materials. For instance, Bhupendra Singh et al. investigated sol–gel-derived $\text{Nd}_{0.65}\text{Ca}_{0.35}\text{MnO}_3$ nanoparticles and observed uniform polycrystalline grains with homogeneous surface texture and elemental distribution, as confirmed by energy-dispersive spectroscopy (EDS)³⁰. Subarna Datta et al. used FE-SEM to reveal a mixture of nanoparticles and nanowires in hydrothermally synthesized $\text{La}_{0.5}\text{Ca}_{0.5}\text{MnO}_3$, demonstrating strong dependence of morphology on parameters such as KOH concentration and reaction time²⁹. Ankit Bhoriya et al. studied Sr-doped $\text{Nd}_{1-x}\text{Sr}_x\text{MnO}_3$ ($x = 0.4, 0.5$) polycrystals and reported dense, irregular grain structures ranging from submicron to several microns, shaped by internal strain and dopant concentration³¹.

Complementing these findings, Raghav et al. systematically explored $\text{La}_{0.15}\text{Pr}_{0.45}\text{Ca}_{0.40}\text{MnO}_3$ (LPCMO) synthesized via the sol–gel route and sintered at temperatures from 600/ °C to 1300/ °C. FE-SEM imaging revealed particle size growth from ~45/ nm to ~370/ nm with higher sintering temperatures, correlating with increased polycrystallinity and evolution of distinct magnetic phases—transitioning from AFM-CO dominance to FM behavior in larger particles³². Similarly, Bingham et al. studied $\text{La}_{0.25}\text{Pr}_{0.375}\text{Ca}_{0.375}\text{MnO}_3$ nanoparticles and demonstrated that below a critical size of ~100/ nm, charge ordering collapses and ferromagnetism becomes dominant, while multiphase coexistence is retained in larger particles³³. Though focused primarily on thermal and magnetic analysis, Han’s study on $\text{Pr}_{0.65}\text{Ca}_{0.35}\text{MnO}_3$ supports these trends by showing the suppression of the AFM state and emergence of FM metallicity under high magnetic fields—further implying size- and strain-dependent phase competition³⁴. Taken together, these FE-SEM studies confirm that surface morphology and grain size in manganite systems are highly sensitive to synthesis methods and composition. Such morphological tuning directly governs the balance of magnetic and electronic phases, making FE-SEM a vital characterization technique in understanding and optimizing the functional behavior of perovskite manganites.

3.3. Magnetic Properties: In low-bandwidth perovskite manganites of the general formula $\text{R}_{1-x}\text{A}_x\text{MnO}_3$ (R = rare-earth, A = alkaline-earth), magnetic behavior is governed by a delicate and complex interplay between multiple coexisting phases—ferromagnetic (FM), antiferromagnetic (AFM), charge-ordered (CO), and spin-glass (SG) states. Studies on $\text{La}_{1-x-y}\text{Pr}_y\text{Ca}_x\text{MnO}_3$ (LPCMO) compounds highlight the critical influence of particle size on phase evolution. Raghav et al. (2021) demonstrated

that in $\text{La}_{0.15}\text{Pr}_{0.45}\text{Ca}_{0.40}\text{MnO}_3$, small particles (~ 45 nm) primarily exhibit FM ordering, while intermediate sizes (~ 139 nm) reveal clear CO and AFM transitions at $T_{\text{CO}} \approx 213$ K and $T_{\text{N}} \approx 173$ K, respectively, with FM emerging at lower temperatures ($T_{\text{C}} \approx 58$ K)³². At larger particle sizes (~ 370 nm), the FM phase regains dominance, with CO/AFM signatures persisting only as magnetic hysteresis. Similar trends were observed by Bingham *et al.* (2012) in $\text{La}_{0.25}\text{Pr}_{0.375}\text{Ca}_{0.375}\text{MnO}_3$, where reduction of particle size below ~ 100 nm suppressed long-range CO/AFM order and enhanced the FM fraction, attributing changes to size-induced strain and surface effects³³. Han (2017) reported that $\text{Pr}_{0.65}\text{Ca}_{0.35}\text{MnO}_3$ exhibits an AFM insulating ground state with cluster-glass characteristics at low temperatures, and under high magnetic fields (≥ 50 kOe), undergoes a CO melting and AFM-to-FM transition accompanied by a drastic drop in resistivity. Specific heat measurements confirmed contributions from both FM and AFM spin waves, indicative of nanoscale magnetic phase coexistence³⁴. Extending this understanding, Raghav *et al.* (2020) found in $\text{La}_{0.30}\text{Pr}_{0.30}\text{Ca}_{0.40}\text{MnO}_3$ that glassy behavior and phase separation become prominent near a particle size of ~ 100 nm, influencing both magnetic and transport properties²⁶. Bhoriya *et al.* (2021) further elaborated on $\text{Nd}_{1-x}\text{Sr}_x\text{MnO}_3$ ($x = 0.4, 0.5$), where temperature-dependent magnetic and Raman studies showed phase separation involving PM, FM, CO, and SG phases, closely coupled with spin-phonon and magnetoelastic interactions³¹. Complementarily, Singh *et al.* (2025) reported in $\text{Nd}_{0.65}\text{Ca}_{0.35}\text{MnO}_3$ that nanoscale effects suppress the insulator–metal transition while preserving PM–FM transitions and glassy magnetic behavior, with FM clusters nucleating in an AFM matrix³⁰. Collectively, these findings underscore the vital role of size, strain, and field effects in controlling the magnetic landscape of LPCMO-type manganites.

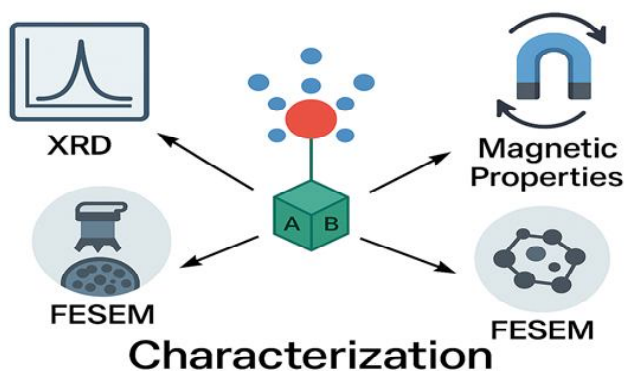


Fig.2. Schematic representation of the characterization techniques used to analyze the synthesized material.

4. Application :

4.1. Photocatalytic: Photocatalytic degradation using perovskite-based nanomaterials has attracted significant attention in recent years due to their efficiency in removing organic pollutants under visible light. Ghiasi and Malekzadeh *et al.* reported the successful synthesis of $\text{La}_{0.70}\text{Sr}_{0.30}\text{MnO}_3$ nanoperovskite via the citrate method, which demonstrated high photocatalytic activity for the degradation of methyl orange under solar irradiation. They found that acidic pH and the presence of

potassium persulfate as an electron acceptor significantly enhanced the degradation rate, and the material showed excellent reusability and stability³⁵. Similarly, Panahi et al. explored the effect of cation (Mn) and anion (N) doping in LaCoO_3 nanoperovskite. The modified materials, $\text{LaCo}_{0.8}\text{Mn}_{0.2}\text{O}_3$ and N-doped LaCoO_3 , exhibited enhanced photocatalytic performance toward malachite green dye under visible light[36]. This improvement was attributed to reduced band gap energy, increased oxygen vacancies, and better charge separation efficiency due to doping. Expanding on the structure-activity relationship, Wang et al. provided a comprehensive review of perovskite-based photocatalysts, highlighting that A-, B-, and X-site substitutions in the perovskite lattice (ABX_3) significantly influence the material's band gap, electron mobility, and surface properties. They emphasized the crucial role of structural distortions, oxygen vacancies, and synthesis methods in tuning photocatalytic performance for degrading gases, dyes, heavy metals, and radionuclides³⁷. More recently, Sharma et al. synthesized $\text{LaFe}_{0.5}\text{Cr}_{0.5}\text{O}_3$ nanoperovskites using a solvent-free combustion-assisted method with various fuels. The sample prepared with urea exhibited the highest BET surface area and showed outstanding degradation of rhodamine B (99% in 60 minutes), as well as effective removal of other dyes like methylene blue and methyl orange. The high performance was linked to its nanoscale size, narrow band gap (2–2.6 eV), visible-light activity, and high structural purity³⁸. Collectively, these studies underline that perovskite oxides, when engineered through controlled doping, compositional tuning, and green synthesis methods, serve as promising and reusable photocatalysts for environmental remediation under solar or visible light conditions.

4.2. Sensor : Nanocrystalline perovskites have emerged as highly promising materials for sensor applications due to their unique optical and electronic properties, structural tunability, and high surface area. Hernández-Rodríguez et al. demonstrated that Nd^{3+} doped yttrium orthoaluminate perovskites exhibit exceptional sensitivity as optical thermal sensors within the near-infrared biological windows, making them suitable for biomedical imaging and sub-tissue thermal sensing applications³⁹. George et al. reviewed the dual capabilities of perovskite nanocrystals in optical and electrochemical sensing, highlighting their fluorescence-based detection of metal ions and gases, along with their redox activity that enables electrochemical sensing strategies⁴⁰. Similarly, Shellaiah and Sun emphasized the versatility of perovskite nanomaterials in chemosensing, including detection of gases like O_2 and CO_2 via current-voltage responses, and the enhancement of sensing performance through doping and formation of nanocomposites⁴¹. Most recently, Bui and Shin provided a comprehensive overview of perovskite-based sensors, noting their rapid photodetection capabilities, sensitivity to humidity, temperature, and toxic gases, and their potential integration into flexible electronic and medical diagnostic platforms despite ongoing challenges related to material stability⁴². Collectively, these studies underscore the vast potential of nanocrystalline perovskites in developing next-generation sensor technologies for environmental and biomedical applications.

4.3. LEDs : Nanocrystalline perovskites have emerged as leading candidates for next-generation light-emitting diode (LED) technologies due to their tunable band gaps, high photoluminescence quantum yields (PLQYs), and solution-processability. Kulkarni et al. highlighted that perovskite quantum dots exhibit PLQYs approaching 100%, owing to enhanced exciton binding energies and suppressed trap states, which significantly improve radiative recombination efficiency in

LEDs⁴³. Moreover, Zhan et al. reported that micro-nano structuring of perovskite layers enhances light extraction efficiency by increasing the optical outcoupling factor, thereby improving the external quantum efficiency (EQE) of perovskite-based LEDs beyond 20%⁴⁴. Recent advances also include the development of one-dimensional perovskite nanorods (PNRs), which possess superior carrier mobility and directional emission, making them highly suitable for polarized and high-efficiency LED applications. Aftab et al. emphasized that PNR-based LEDs demonstrate enhanced light emission performance, attributed to their anisotropic geometry and improved charge transport, offering promising routes toward solid-state lighting and advanced display technologies⁴⁵. These findings underscore the significant progress and potential of nanocrystalline perovskites, especially in LED applications, where their structural and compositional tunability can be harnessed to optimize device efficiency and color purity.

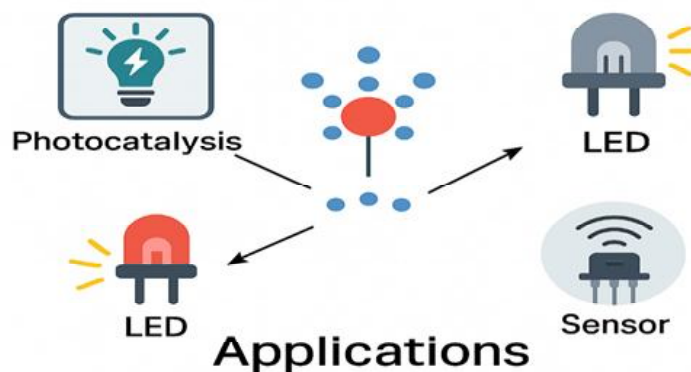


Fig. 3. Applications of thenanocrystalline perovskite material include photocatalysis, LEDs, and sensors.

5. Conclusion :

Nanocrystalline perovskite materials, particularly rare-earth manganese oxides and their doped derivatives (manganites), continue to attract significant research interest due to their rich electronic phase diagrams and multifunctional properties. The remarkable phenomena such as colossal magnetoresistance (CMR), charge ordering, and phase separation offer deep insights into the interplay of structural, magnetic, and electronic phases in these systems. Advances in nanostructuring have opened new possibilities, allowing perovskite materials to exhibit size-dependent magnetic transitions, enhanced surface reactivity, and improved phase stability. Diverse synthesis methods—such as sol-gel, hydrothermal, and chemical precipitation enable precise control over particle size, crystallinity, and morphology, which in turn influence the materials' magnetic, electrical, and catalytic behaviors. Characterization techniques like XRD and FE-SEM further facilitate detailed investigation of structural evolution and morphology. Studies confirm that reduced dimensions and controlled doping induce complex phase transitions between FM, AFM, and CO states, leading to tailored magnetic and transport properties. Importantly, nanocrystalline perovskites have demonstrated exceptional versatility in applications ranging from photocatalysis and chemical sensing to next-generation optoelectronic devices like LEDs. Their high surface area, tunable bandgap, and solution-processability make them strong candidates for solar-driven environmental remediation, biomedical sensing, and solid-state lighting.

Despite these advances, challenges remain in enhancing material stability, controlling phase purity, and scaling up fabrication processes for commercial applications.

Scope of Future Work :

Future research should focus on eco-friendly synthesis strategies, real-time phase monitoring, and integration into flexible device architectures to fully harness the potential of these multifunctional perovskite materials.

References :

1. A.P. Ramirez, Colossal magnetoresistance, *J. Phys. Condens. Matter* 9 (1997) 8171–8199. <https://doi.org/10.1088/0953-8984/9/39/005>.
2. Y. Tokura, Critical features of colossal magnetoresistive manganites, *Reports Prog. Phys.* 69 (2006) 797–851. <https://doi.org/10.1088/0034-4885/69/3/R06>.
3. P.K. Siwach, H.K. Singh, O.N. Srivastava, Low field magnetotransport in manganites, *J. Phys. Condens. Matter* 20 (2008) 273201. <https://doi.org/10.1088/0953-8984/20/27/273201>.
4. E. Dagotto, Open questions in CMR manganites, relevance of clustered states and analogies with other compounds including the cuprates, *New J. Phys.* 7 (2005) 67–67. <https://doi.org/10.1088/1367-2630/7/1/067>.
5. E. Dagotto, T. Hotta, A. Moreo, Colossal magnetoresistant materials: the key role of phase separation, *Phys. Rep.* 344 (2001) 1–153. [https://doi.org/10.1016/S0370-1573\(00\)00121-6](https://doi.org/10.1016/S0370-1573(00)00121-6).
6. E. Dagotto, *Nanoscale Phase Separation and Colossal Magnetoresistance*, Springer Berlin Heidelberg, Berlin, Heidelberg, 2003. <https://doi.org/10.1007/978-3-662-05244-0>.
7. R. von Helmolt, J. Wecker, B. Holzapfel, L. Schultz, K. Samwer, Giant negative magnetoresistance in perovskitelike $\text{La}_{2/3}\text{Ba}_{1/3}\text{MnO}_x$ ferromagnetic films, *Phys. Rev. Lett.* 71 (1993) 2331–2333. <https://doi.org/10.1103/PhysRevLett.71.2331>.
8. E. Burzo, I.G. Pop, D.N. Kozlenko, Magnetic and magnetocaloric properties of some ferrimagnetic compounds, *J. Optoelectron. Adv. Mater.* 12 (2010) 1105–1113.
9. Q.H. Lu, K.L. Yao, D. Xi, Z.L. Liu, X.P. Luo, Q. Ning, Synthesis and characterization of composite nanoparticles comprised of gold shell and magnetic core/cores, *J. Magn. Magn. Mater.* 301 (2006) 44–49. <https://doi.org/10.1016/j.jmmm.2005.06.007>.
10. G. Whitesides, Nanoscience, Nanotechnology, and Chemistry, *Small* 1 (2005) 172–179. <https://doi.org/10.1002/smll.200400130>.
11. Z.L. Wang, Nanopiezotronics, *Adv. Mater.* 19 (2007) 889–892. <https://doi.org/10.1002/adma.200602918>.
12. D. Jena, A. Konar, Enhancement of Carrier Mobility in Semiconductor Nanostructures by Dielectric Engineering, *Phys. Rev. Lett.* 98 (2007) 136805. <https://doi.org/10.1103/PhysRevLett.98.136805>.
13. V. Bedekar, O.D. Jayakumar, J. Manjanna, A.K. Tyagi, Synthesis and magnetic studies of nanocrystalline GdFeO_3 , *Mater. Lett.* 62 (2008) 3793–3795. <https://doi.org/10.1016/j.matlet.2008.04.053>.
14. R.W. Siegel, G.E. Fougere, Mechanical properties of nanophase metals, *Nanostructured Mater.* 6 (1995) 205–216. [https://doi.org/10.1016/0965-9773\(95\)00044-5](https://doi.org/10.1016/0965-9773(95)00044-5).
15. C.N.R. Rao, P.V. Vanitha, Phase separation and segregation in rare earth manganates: the experimental situation, *Curr. Opin. Solid State Mater. Sci.* 6 (2002) 97–106. [https://doi.org/10.1016/S1359-0286\(02\)00035-9](https://doi.org/10.1016/S1359-0286(02)00035-9).

16. J.R. Chocha, P.A. Chhelavda, J.A. Bhalodia, Calcination temperature effect on $\text{La}_{0.67}\text{Ca}_{0.33}\text{MnO}_3$ nanoparticle using simple citrate pyrolysis process, *Trans. Indian Inst. Met.* 64 (2011) 159–163. <https://doi.org/10.1007/s12666-011-0031-7>.
17. Y. Wang, P. Chen, M. Liu, Synthesis of well-defined copper nanocubes by a one-pot solution process, *Nanotechnology* 17 (2006) 6000–6006. <https://doi.org/10.1088/0957-4484/17/24/016>.
18. N. Pinna, M. Willinger, K. Weiss, J. Urban, R. Schlögl, Local Structure of Nanoscopic Materials: V_2O_5 Nanorods and Nanowires, *Nano Lett.* 3 (2003) 1131–1134. <https://doi.org/10.1021/nl034326s>.
19. L. Yan, F. Bai, J. Li, D. Viehland, Nanobelt Structure in Perovskite-Spinel Composite Thin Films, *J. Am. Ceram. Soc.* 92 (2009) 17–20. <https://doi.org/10.1111/j.1551-2916.2008.02825.x>.
20. Y. Ebina, T. Sasaki, M. Harada, M. Watanabe, Restacked Perovskite Nanosheets and Their Pt-Loaded Materials as Photocatalysts, *Chem. Mater.* 14 (2002) 4390–4395. <https://doi.org/10.1021/cm020622e>.
21. R. Ma, Y. Bando, T. Sato, Nanowires of metal borates, *Appl. Phys. Lett.* 81 (2002) 3467–3469. <https://doi.org/10.1063/1.1517178>.
22. Y. Mao, S. Banerjee, S.S. Wong, Hydrothermal synthesis of perovskite nanotubes, *Chem. Commun.* (2003) 408–409. <https://doi.org/10.1039/b210633g>.
23. D.M. Newns, Junction mott transition field effect transistor (JMTFET) and switch for logic and memory applications, US006121642A, 2000.
24. A. Srinivas, R. Gopalan, V. Chandrasekharan, Room temperature multiferroism and magnetoelectric coupling in system, *Solid State Commun.* 149 (2009) 367–370. <https://doi.org/10.1016/j.ssc.2008.12.013>.
25. R.D. Shull, A.J. Shapiro, V.S. Gornakov, V.I. Nikitenko, J.S. Jiang, H. Kaper, G. Leaf, S.D. Bader, Spin spring behavior in exchange coupled soft and high-coercivity hard ferromagnets, *IEEE Trans. Magn.* 37 (2001) 2576–2578. <https://doi.org/10.1109/20.951240>.
26. D.S. Raghav, S. Kumari, H.K. Singh, G.D. Varma, Structure, magnetism and electrical transport of sol-gel derived $\text{La}_{0.30}\text{Pr}_{0.30}\text{Ca}_{0.40}\text{MnO}_3$: Elucidating consequences of size effect, *J. Magn. Mater.* 497 (2020) 166003. <https://doi.org/10.1016/j.jmmm.2019.166003>.
27. L.C. Mno, S.S. Kekade, R.S. Devan, A. V Deshmukh, D.M. Phase, R.J. Choudhary, S.I. Patil, Electron transport behavior and charge ordering phenomena in, *J. Alloys Compd.* 682 (2016) 447–453. <https://doi.org/10.1016/j.jallcom.2016.05.003>.
28. W. Xia, L. Li, H. Wu, P. Xue, X. Zhu, Structural, morphological, and magnetic properties of sol-gel derived $\text{La}_{0.7}\text{Ca}_{0.3}\text{MnO}_3$ manganite nanoparticles, *Ceram. Int.* 43 (2017) 3274–3283. <https://doi.org/10.1016/j.ceramint.2016.11.160>.
29. S. Datta, A. Ghatak, B. Ghosh, Manganite ($\text{La}_{1-x}\text{A}_x\text{MnO}_3$; A = Sr, Ca) nanowires with adaptable stoichiometry grown by hydrothermal method/ : understanding of growth mechanism usin ... Manganite ($\text{La}_{1-x}\text{A}_x\text{MnO}_3$; A = Sr, Ca) nanowires with adaptable stoichiometry grown by hydrothermal method/ : understanding of growth mechanism using spatially resolved techniques, *J. Mater. Sci.* 51 (2016) 9679–9695. <https://doi.org/10.1007/s10853-016-0201-4>.
30. S. Gel, D. Nd, C. Mno, B. Singh, G. Joshi, S. Tomar, U. Kumar, L. Kumar, R. Kumar, Exploring Structural, Magnetic, and Electric Transport, 2025 (2025) 11–13. <https://doi.org/10.1155/acmp/8318984>.
31. A. Bhoriya, D.S. Raghav, N. Bura, D. Yadav, J. Singh, H.K. Singh, N. Dilawar Sharma, Probing

- phase separation in $\text{Nd}_{1-x}\text{Sr}_x\text{MnO}_3$ ($x \approx 0.4, 0.5$) polycrystals through temperature dependent magnetic and Raman spectroscopy studies, *J. Alloys Compd.* 894 (2022) 162424. <https://doi.org/10.1016/j.jallcom.2021.162424>.
32. D.S. Raghav, S. Kumari, H.K. Singh, P.K. Siwach, G.D. Varma, Evolution of the magnetic and charge orders in $\text{La}_{0.15}\text{Pr}_{0.45}\text{Ca}_{0.40}\text{MnO}_3$: Assessing the role of particle size and magnetic field, *J. Magn. Magn. Mater.* 536 (2021) 168126. <https://doi.org/10.1016/j.jmmm.2021.168126>.
 33. N.S. Bingham, P. Lampen, M.H. Phan, T.D. Hoang, H.D. Chinh, C.L. Zhang, S.W. Cheong, H. Srikanth, Impact of nanostructuring on the magnetic and magnetocaloric properties of microscale phase-separated $\text{La}_{5/8}\text{yPr}_{3/8}\text{Ca}_{3/8}\text{MnO}_3$ manganites, *Phys. Rev. B* 86 (2012) 064420. <https://doi.org/10.1103/PhysRevB.86.064420>.
 34. Z. Han, The low temperature specific heat and electrical transport, magnetic properties of $\text{Pr}_{0.65}\text{Ca}_{0.35}\text{MnO}_3$, *J. Magn. Magn. Mater.* 423 (2017) 171–174. <https://doi.org/10.1016/j.jmmm.2016.09.083>.
 35. M. Ghiasi, A. Malekzadeh, Solar photocatalytic degradation of methyl orange over $\text{La}_{0.7}\text{Sr}_{0.3}\text{MnO}_3$ nano-perovskite, *Sep. Purif. Technol.* 134 (2014) 12–19. <https://doi.org/10.1016/j.seppur.2014.07.022>.
 36. P.N. Panahi, S. Babaei, M.H. Rasoulifard, Photocatalytic activity of cation (Mn) and anion (N) substitution in LaCoO_3 nanoperovskite under visible light, *Rare Met.* 39 (2020) 139–146. <https://doi.org/10.1007/s12598-019-01329-9>.
 37. H. Wang, Q. Zhang, M. Qiu, B. Hu, Synthesis and application of perovskite-based photocatalysts in environmental remediation/ : A review, *J. Mol. Liq.* 334 (2021) 116029. <https://doi.org/10.1016/j.molliq.2021.116029>.
 38. S. Sharma, I. Qadir, A.K. Atri, S. Singh, U. Manhas, D. Singh, Nanostructures for Excellent Photocatalytic Performance toward Water Decontamination/ : The Effect of Fuel on Structural , Magnetic, and Photocatalytic Properties, (2023). <https://doi.org/10.1021/acsomega.2c05594>.
 39. M.A. Hernández-rodríguez, A.D. Lozano-gorrín, I.R. Martín, Sensors and Actuators B/ : Chemical Comparison of the sensitivity as optical temperature sensor of nano-perovskite doped with Nd^{3+} ions in the first and second biological windows, *Sensors Actuators B. Chem.* 255 (2018) 970–976. <https://doi.org/10.1016/j.snb.2017.08.140>.
 40. J.G. K, V. V Halali, C.G. Sanjayan, V. Suvina, M. Sakar, R.G. Balakrishna, INORGANIC CHEMISTRY FRONTIERS Perovskite nanomaterials as optical and electrochemical sensors, (2020) 2702–2725. <https://doi.org/10.1039/d0qi00306a>.
 41. M. Shellaiah, Review on Sensing Applications of Perovskite Nanomaterials, (2020).
 42. T.H. Bui, J.H. Shin, Perovskite materials for sensing applications/ : Recent advances and challenges, *Microchem. J.* 191 (2023) 108924. <https://doi.org/10.1016/j.microc.2023.108924>.
 43. S.A. Kulkarni, S.G. Mhaisalkar, N. Mathews, P.P. Boix, Perovskite Nanoparticles/ : Synthesis, Properties, and Novel Applications in Photovoltaics and LEDs, 1800231 (2019) 1–16. <https://doi.org/10.1002/smtd.201800231>.
 44. Y. Zhan, Q. Cheng, Y. Song, M. Li, Micro-Nano Structure Functionalized Perovskite Optoelectronics/ : From Structure Functionalities to Device Applications, 2200385 (2022) 1–32. <https://doi.org/10.1002/adfm.202200385>.
 45. S. Aftab, X. Li, F. Kabir, E. Akman, M. Aslam, M. Reddy, G. Koyyada, M.A. Assiri, Nano Energy Lighting the future/ : Perovskite nanorods and their advances across applications, *Nano Energy* 124 (2024) 109504. <https://doi.org/10.1016/j.nanoen.2024.109504>.